Imaging Science in Dentistry 2023; 53: 27-34
https://doi.org/10.5624/isd.20220133

Effect of deep transfer learning with a different kind of lesion on classification performance of pre-trained model: Verification with radiolucent lesions on panoramic radiographs

Yoshitaka Kise[1,*], Yoshiko Ariji[2], Chiaki Kuwada[1], Motoki Fukuda[1], Eiichiro Ariji[1]

[1]*Department of Oral and Maxillofacial Radiology, Aichi Gakuin University School of Dentistry, Nagoya, Japan*
[2]*Department of Oral Radiology, Osaka Dental University, Osaka, Japan*

ABSTRACT

Purpose: The aim of this study was to clarify the influence of training with a different kind of lesion on the performance of a target model.

Materials and Methods: A total of 310 patients (211 men, 99 women; average age, 47.9 ± 16.1 years) were selected and their panoramic images were used in this study. We created a source model using panoramic radiographs including mandibular radiolucent cyst-like lesions (radicular cyst, dentigerous cyst, odontogenic keratocyst, and ameloblastoma). The model was simulatively transferred and trained on images of Stafne's bone cavity. A learning model was created using a customized DetectNet built in the Digits version 5.0 (NVIDIA, Santa Clara, CA). Two machines (Machines A and B) with identical specifications were used to simulate transfer learning. A source model was created from the data consisting of ameloblastoma, odontogenic keratocyst, dentigerous cyst, and radicular cyst in Machine A. Thereafter, it was transferred to Machine B and trained on additional data of Stafne's bone cavity to create target models. To investigate the effect of the number of cases, we created several target models with different numbers of Stafne's bone cavity cases.

Results: When the Stafne's bone cavity data were added to the training, both the detection and classification performances for this pathology improved. Even for lesions other than Stafne's bone cavity, the detection sensitivities tended to increase with the increase in the number of Stafne's bone cavities.

Conclusion: This study showed that using different lesions for transfer learning improves the performance of the model. ***(Imaging Sci Dent 2023; 53: 27-34)***

KEY WORDS: Deep Learning; Machine Learning; Jaw Diseases; Radiography, Panoramic

Introduction

In recent years, artificial intelligence (AI) created by deep learning (DL) systems with convolutional neural networks (CNN) has received significant attention and can be applied to imaging diagnosis in the field of oral and maxillofacial radiology.[1-12] Although many research articles have reported good performance with this application, several problems remain to be addressed before a model suitable for clinical use is achieved. Large amounts of qualified data are required to create a high-performance learning model, and it is difficult to collect sufficient data from an institution, especially for relatively rare diseases. Use of the transfer learning method is one solution to this problem. In a broad sense, a CNN that has already been trained on various kind of images is additionally trained on a relatively small range of images to create an effective model for specific purposes. For example, training on medical images of certain pathologies is additionally performed using a CNN pretrained on an image database openly available on the internet, such as ImageNet, to create an effective model for these pathologies. Some CNNs, such as VGG-16[13] and GoogLeNet,[14] are such pretrained CNNs. More specifically, with this method, a model that is created in an institution and assigned as a source model can

Received July 25, 2022; Revised October 28, 2022; Accepted October 31, 2022
Published online November 30, 2022
*Correspondence to : Dr. Yoshitaka Kise
Department of Oral and Maxillofacial Radiology, Aichi Gakuin University School of Dentistry, 2-11 Suemori-dori, Chikusa-ku, Nagoya 464-8651, Japan
Tel) 81-527592165, E-mail) kise@dpc.agu.ac.jp

Imaging Science in Dentistry · pISSN 2233-7822 eISSN 2233-7830

be transferred to another institution without transferring the personal data of patients. Thereafter, the transferred pre-trained model is trained on data obtained in another institution and a new model is developed. This new model is called the "target model". Accordingly, the exposure of personal information can be avoided and the target model can be created with relatively small amounts of data obtained in the institution to which the source model is transferred.[15] Several studies have addressed the efficacy of this method for diagnosing certain diseases, such as maxillary sinusitis[16] and sialoliths,[17] on panoramic radiographs. Although effective target models could be created in these studies with a relatively small number of datasets, the additional datasets included the same diseases and conditions used for creating the source models. Indeed, the disease type distribution differs among hospitals depending on their characteristics. A target model should be customized according to the hospital's circumstances. In some cases, therefore, different kinds of diseases may be used for transfer learning. According to the concept and characteristics of the transfer learning procedure, the performance of the target model would be improved in diagnosing both pathologies (one used for initially creating the source model and one used for additional transferred learning). However, the efficacy of the models has not been verified for diagnosis via panoramic radiographs.

The aim of the present study was to clarify the influence of training with a different kind of lesion on the performance of the target model. For this aim, a source model was created using panoramic radiographs with mandibular radiolucent cyst-like lesions (ameloblastoma, odontogenic keratocyst, dentigerous cyst, and radicular cyst) in a similar manner to that of a previous study,[18] and the model was thereafter simulatively transferred and trained on images of Stafne's bone cavity.

Materials and Methods

The study design was approved by the Ethics Committee of Aichi Gakuin University (approval number 496) and was planned according to the ethical standards of the Helsinki Declaration. Informed consent was obtained from all patients for inclusion in the study.

Participants

The participants were retrospectively selected from an image database of patients who visited our institution from 2000 to 2021. Patients with cyst-like radiolucent lesions in the mandible were included. Patients with a history of previous surgery or malignant lesions were excluded. A total of 310 patients (211 men, 99 women; average age, 47.9 ± 16.1 years) were selected and their panoramic images were used in this study (Table 1). The lesions included 38 ameloblastomas, 41 odontogenic keratocysts, 82 dentigerous cysts, 84 radicular cysts, and 65 cases of Stafne's bone cavity. All lesions except the Stafne's bone cavities had confirmed histopathological diagnoses. For the cases of Stafne's bone cavity that did not require aggressive treatment, two radiologists with more than 10 years' experience made the diagnosis based on the computed tomography appearance after reaching a consensus. Cases were randomly assigned to the training datasets (80%) and the test dataset (20%). Then, 20% of the training data were randomly assigned as validation data.

Imaging data

The digital panoramic radiographs of all the patients were obtained using a Veraview Epocs system (J Morita Mfg Corp, Kyoto, Japan). The standard parameters were tube voltage 75 kV, tube current 9 mA, and acquisition time 16 seconds.

Table 1. Summary of subjects and number of training, validation, and test datasets

	No. of patients	Age	Training dataset	Validation dataset	Test dataset
Ameloblastoma	38	42.4 ± 20.4	25	6	7
Odontogenic keratocyst	41	43.8 ± 16.4	26	7	8
Dentigerous cyst	82	46.6 ± 11.4	53	13	16
Radicular cyst	84	44.7 ± 14.3	54	14	16
Stafne's bone cavity	65	59.7 ± 14.8	42	10	13
Total	310	47.9 ± 16.1	200	50	60

Selected images were downloaded from the hospital imaging database in tagged image file format (TIFF). A single radiologist converted them from TIFF format to portable network graphics format (PNG). Therefore, all images used in this study were uncompressed. Next, all images were cropped to a size of 900 × 900 pixels to adapt to the Detect Net standard used in this verification.

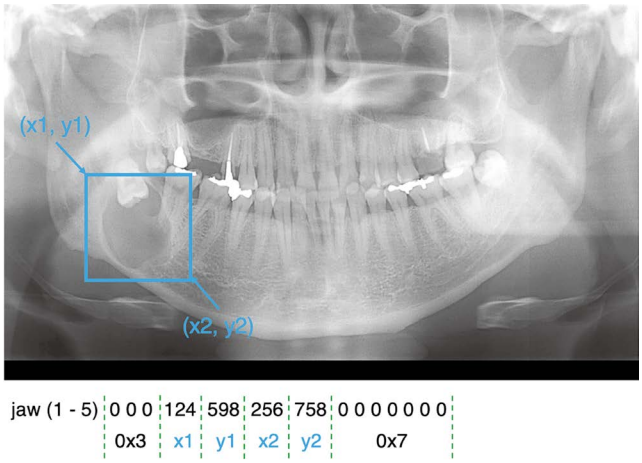

Fig. 1. A rectangular region of interest (bounding box in blue) of an arbitrary size is set for the lesion, and the coordinates of the upper left corner (x1, y1) and the lower right corner (x2, y2) are recorded. The labels are then created in text format.

Labeling procedure

A labeling procedure was performed on the images. Labels containing the type of lesion (class name) and the coordinates of the lesion were created in text format. The class names of the lesions were determined as jaw1 for ameloblastomas, jaw2 for odontogenic keratocysts, jaw3 for dentigerous cysts, jaw4 for radicular cysts, and jaw5 for Stafne's bone cavities. The coordinates of the upper left and lower right corners of the square regions of interest surrounding the lesions were recorded for each image (Fig. 1).

Deep learning system

The deep learning process was implemented on an NVIDIA GeForce GTX GPU workstation (Nvidia Corp., Santa Clara, CA, USA) with 11 GB of GPU and 128 GB of memory. We used the DetectNet network for object detection on the DIGITS training system version 5.0 (NVIDIA, Santa Clara, CA; https://developer.ndivia.com/digits) and the Caffe framework, and used the adaptive moment estimation (Adam) solver, with 0.0001 as the base learning rate

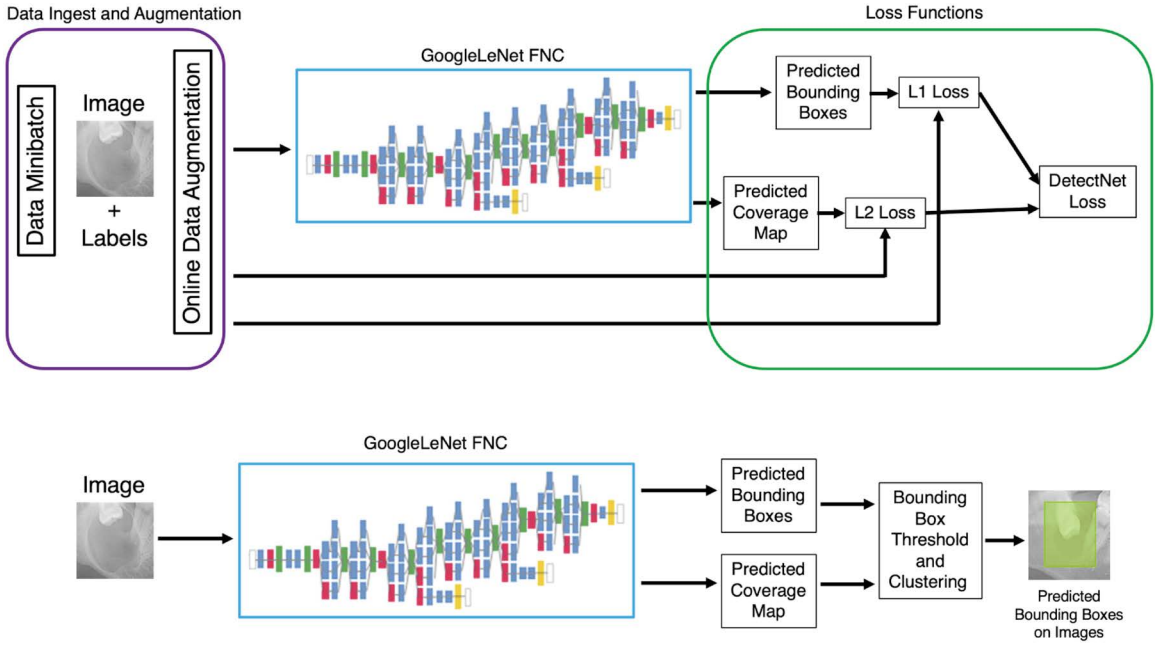

Fig. 2. DetectNet architecture. Data layers ingest 4 or 5 training images and labels, and transformer layers perform inline data augmentation. A fully convolutional network (FCN) performs feature extraction and prediction of object classes and bounding boxes per grid square. Loss functions simultaneously measure the error in the two tasks of predicting the object coverage (L2 loss) and object bounding box corners per grid square (L1 loss). Testing processes are shown in the bottom row. A clustering function produces the final set of predicted bounding boxes during the testing processes. The predicted bounding box is the area in which the learning model predicts the presence of a lesion. When the presence of a radiolucent lesion is predicted, the colored bounding boxes are superimposed over the panoramic radiographs. The threshold value was set at 0.6.

(Fig. 2). The training processes were conducted for 1000 epochs, and a learning model was obtained. The fully convolutional network (FCN) sub-network of DetectNet has the same structure as GoogLeNet without the data input layers, final pooling layer, and output layers, and we used a pretrained GoogLeNet model in this study.[19,20]

Learning model creation

Two machines (Machines A and B) with identical specifications were used to simulate transfer learning (Fig. 3). A source model was created from the data consisting of ameloblastoma, odontogenic keratocyst, dentigerous cyst, and radicular cyst in Machine A. Thereafter, it was transferred to Machine B and trained on additional data of Stafne's bone cavity to create target models. To investigate the effect of the number of cases, several target models were created with different numbers of Stafne's bone cavity cases. Three target models (T10, T21 and T42) were created by training the transferred source model using 10, 21 and 42 images of Stafne's bone cavity. T0 denotes the source model that was transferred but not trained.

Learning model performance

The source model was evaluated with test data including the four lesions, which created the model as a benchmark, while the target model's performance was assessed with test data including these four lesions and additional Stafne's bone cavity data (Fig. 3). When the presence of a radiolucent lesion was predicted by the models, the colored bounding boxes were superimposed over the panoramic images with different colors according to the classification of the lesion (Fig. 4). The predicted bounding boxes were displayed in red, light blue, green, purple, and yellow for jaw1 (ameloblastoma), jaw2 (odontogenic keratocyst), jaw3 (dentigerous cyst), jaw4 (radicular cyst), and jaw5 (Stafne's bone cavity), respectively.

Intersection over Union (IoU), which is the most popular evaluation metric used in object detection, was calculated based on the predicted and ground truth areas. In this study, the IoU threshold for determining whether the lesions could be correctly detected was set at 0.6. The ground truth was determined by an experienced radiologist in a manner similar to the establishment of the region of interest in the labeling procedure (blue square in Fig. 1).

To evaluate the performance of lesion detection, the detection sensitivity was calculated as the ratio of the number of correctly predicted areas out of the areas actually including the lesions regardless of their classification. Furthermore, the classification sensitivity was calculated with respect to the lesions that could be correctly detected as the ratio of the number of correctly classified lesions divided by the number of verified lesions. The accuracy and specificity of each model were also calculated.

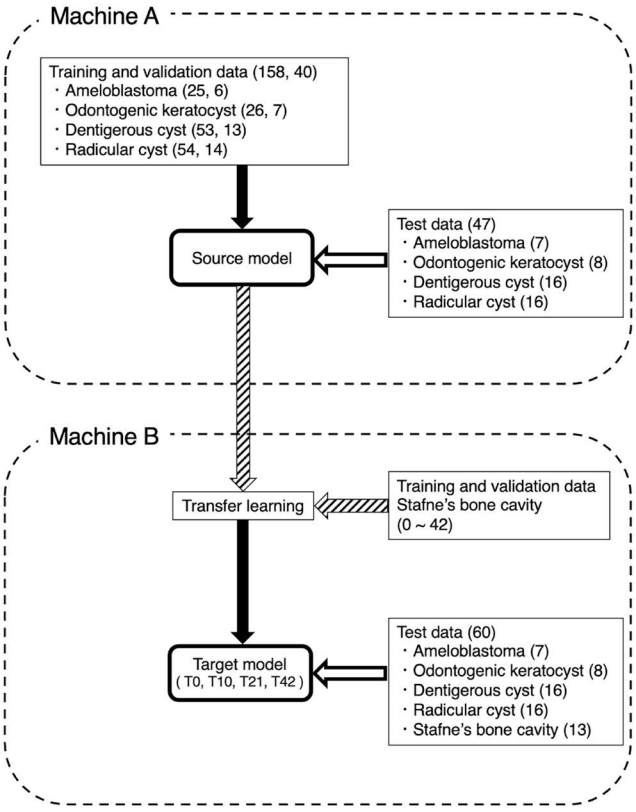

Fig. 3. Diagram of study design. Machine A: The process of creating a source model using four lesions (ameloblastoma, odontogenic keratocyst, dentigerous cyst, and radicular cyst). Machine B: The process of creating the target model by transfer learning a case of Stafne's bone cavity to the source model. Target models (Tn) are created by training the transferred source model using n image patches of Stafne's bone cavity. T0 denotes a source model that is transferred but not trained.

Results

Summaries of the detection and classification performances of each model are shown in Tables 2 and 3. The T0 target model that was not trained on the Stafne's bone cavity data could not detect this pathology as a natural result. When the Stafne's bone cavity data were added to the training, both the detection and classification performances for this pathology improved. Even for lesions other than Stafne's bone cavity, the detection sensitivities tended to increase with the increase in the number of Stafne's bone cavities. Compared with the source model as a benchmark, the classification sensitivity of the T42 model was higher

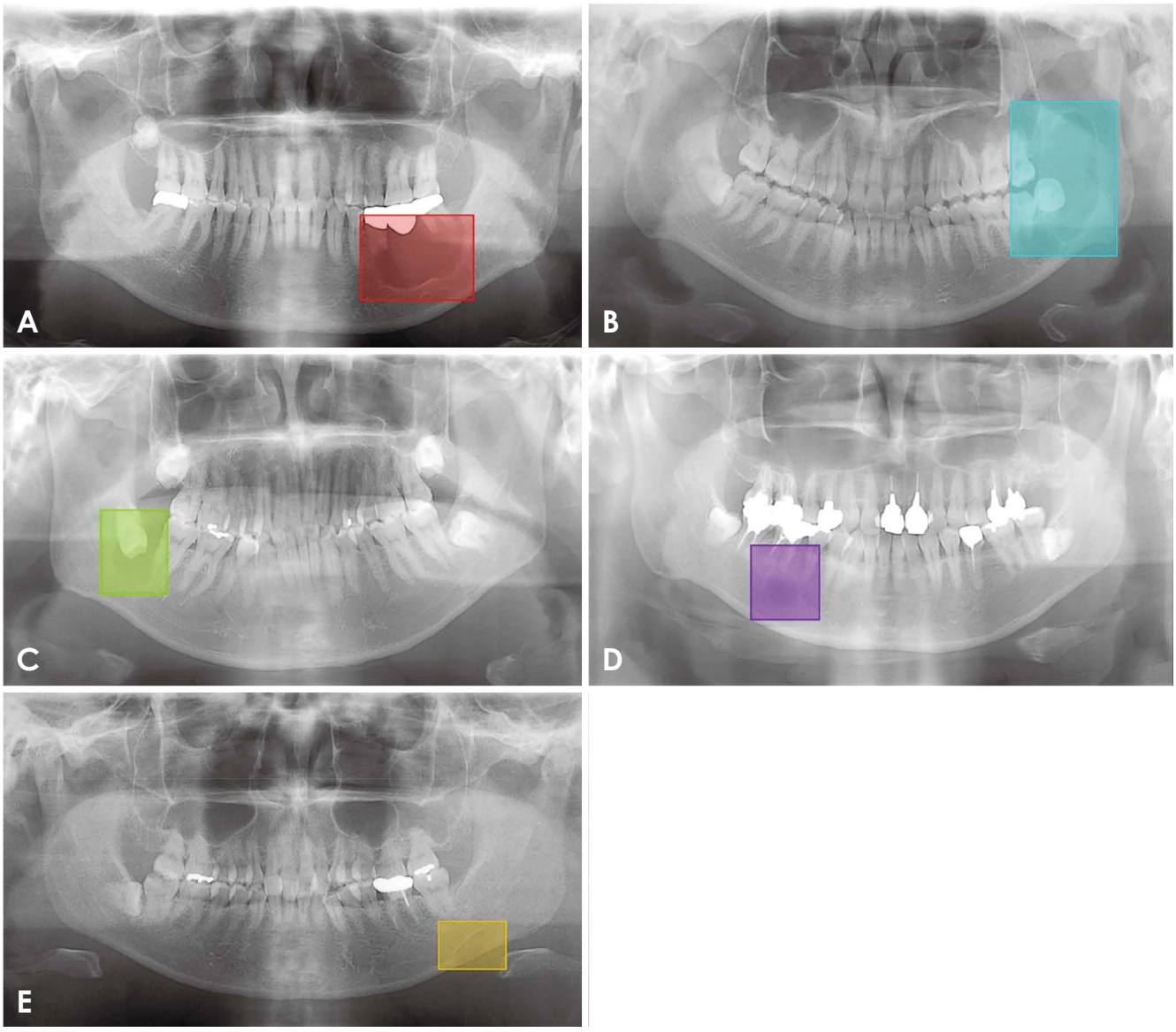

Fig. 4. Examples of successful classification of lesions. The predicted bounding boxes are displayed in red for ameloblastoma (A), in light blue for odontogenic keratocyst (B), in green for dentigerous cyst (C), in purple for radicular cyst (D), and in yellow for Stafne's bone cavity (E).

Table 2. Detection sensitivity of each model

Lesion	Source model*	Target model**			
		T0	T10	T21	T42
Ameloblastoma	0.57	0.57	0.57	0.86	0.71
Odontogenic keratocyst	0.88	0.88	0.88	0.63	0.88
Dentigerous cyst	1.00	1.00	1.00	1.00	1.00
Radicular cyst	0.63	0.63	0.69	0.75	0.75
Stafne's bone cavity	–	0.00	0.69	0.69	0.92
Total	0.79	0.65	0.78	0.80	0.87

*: source model is created and tested with data not including Stafne's bone cavity as a benchmark. **: target models (Tn) are created by training the transferred source model using n image patches of Stafne's bone cavity and were tested with data including all 5 kinds of lesions. T0 denotes a source model that was transferred but not trained.

Table 3. Classification performances of each model

Lesion	Performance indices	Source model*	Target model**			
			T0	T10	T21	T42
Ameloblastoma	Sensitivity	0.50	0.50	0.75	0.67	0.80
	Specificity	1.00	0.97	0.91	0.95	0.96
	Accuracy	0.95	0.92	0.89	0.92	0.94
Odontogenic keratocyst	Sensitivity	0.29	0.29	0.29	0.40	0.57
	Specificity	0.93	0.94	0.98	0.98	0.98
	Accuracy	0.81	0.82	0.87	0.92	0.92
Dentigerous cyst	Sensitivity	1.00	1.00	0.88	1.00	1.00
	Specificity	0.90	0.87	0.94	0.94	1.00
	Accuracy	0.95	0.92	0.91	0.96	1.00
Radicular cyst	Sensitivity	0.90	0.90	0.91	0.83	0.83
	Specificity	0.85	0.86	0.94	0.97	0.93
	Accuracy	0.86	0.87	0.94	0.94	0.90
Stafne's bone cavity	Sensitivity	–	0.00	1.00	1.00	0.92
	Specificity	–	1.00	1.00	0.97	0.98
	Accuracy	–	0.95	1.00	0.98	0.96
Overall accuracy		0.89	0.90	0.92	0.94	0.95

*: source model is created and tested with data not including Stafne's bone cavity as a benchmark. **: target models (Tn) are created by training the transferred source model using n image patches of Stafne's bone cavity and were tested by data including all 5 kinds of lesions. T0 denotes a source model that was transferred but not trained.

for the lesions of ameloblastoma and odontogenic keratocyst, but was equivalent or slightly lower for dentigerous and radicular cysts. The overall accuracy was higher for the T42 model than for the other models.

Discussion

The DetectNet network used in the present study was developed based on GoogLeNet, which is known as a pre-trained CNN with images of various kinds other than medical images.[14,19,20] The present study, however, aimed to assess the use of a transfer learning procedure in a more specific sense. We evaluated the efficacy of a method of transferring a source to create target models with a relatively small amount of data and without disclosing patients' personal data.[15] Several previous reports have examined the usefulness of this method on panoramic radiographs. Mori et al.[16] created effective models using transfer learning for the detection of maxillary sinuses and diagnosis of maxillary sinusitis on panoramic radiographs. They reported that their detection and classification sensitivity exceeded 0.9 with transfer learning, reaching a satisfactory diagnostic performance. Ishibashi et al.[17] compared the performance of three learning models, including a model created with the transfer learning method, in detecting submandibular gland sialoliths on panoramic radiographs. They concluded that transfer learning with appropriate learning epochs could improve performance in detecting submandibular gland sialoliths on panoramic radiographs. Furthermore, they emphasized the use of the transfer learning method as an alternative to sharing radiographs and patients' personal data among institutions. Although effective target models could be created in these studies with a relatively small number of datasets using a transfer learning technique, the additional datasets included the same diseases used for creating the source models.

This study used 5 types of radiolucent lesions in the mandible and first created a source model trained on four lesions (ameloblastoma, odontogenic keratocyst, dentigerous cyst, and radicular cyst). The source model was then transferred and trained with Stafne's bone cavity cases to create a target model and its sensitivity was compared with the source model. When the source model was transferred and trained even with data of a different lesion (Stafne's bone cavity), overall detection sensitivity tended to increase together with that of the other lesions. Furthermore, classification

sensitivity also tended to increase for ameloblastoma and odontogenic keratocyst. These results suggest that the performance of the target model may improve with the increase in training data, even if the data used for training were different. Therefore, by using the target model, in addition to the advantage of reducing the risk of personal information leakage and increasing the number of cases by being able to use it at multiple facilities, the performance of the model is improved even when different lesions are used for training. This makes it even more useful to share models between institutions, and has the potential to improve model performance with each use.

Dentigerous cyst, radicular cyst, and Stafne's bone cavity showed high classification sensitivity in all models. This indicated that these lesions had characteristic radiographic features and might be easily recognized by the AI system. However, the classification sensitivity of odontogenic keratocyst (0.29-0.50) was lower than that of the other lesions in spite of the increment of this lesion's number, indicating unsatisfactory performance. Odontogenic keratocyst is a relatively common radiolucent lesion, and its imaging features may frequently overlap with those of other lesions.[21-25] Indeed, ameloblastomas and dentigerous cysts are thought to be difficult to differentiate from odontogenic keratocysts. However, classification sensitivity tended to improve as the number of cases used for transfer training increased. Therefore, we suggest that further improvement in classification sensitivity could be expected with a larger number of cases even including different kinds of lesions.

Using a deep learning algorithm, Lee et al.[4] reported good performance with 99.25% accuracy for differentiating Stafne's bone cavity from cysts and tumors of the jaw on panoramic radiographs. Although the main aim of the present study was different from theirs, our results support their conclusion indicating that the characteristic features of Stafne's bone cavity,[4,26] such as location, might contribute to the good performance.

The present study had several limitations. First, this study used only 1 type of neural network (DetectNet). There are several neural networks, such as YOLO[8] and Faster R-CNN,[27] used in object detection techniques. The results of the present study should be verified with comparison to these networks in the future. Second, all images used in the present study were taken with the same equipment at the same facility. This was a drawback; however, it allowed us to investigate the effects caused solely by differences in the types of lesions. Third, no cases of radiopaque lesions were included. This study used only radiolucent lesions, which might have yielded good results. Therefore, the impact of using radiopaque lesions as the material for transfer learning in the model required to be investigated. Finally, the number of patients was too small and there were variations in the number of cases. The number of cases used for training is one factor that affects the performance of the model. In this study, there were fewer ameloblastomas and odontogenic keratocysts, and the results were lower for these lesions than for the other cases. This might have occurred because of the variability in the number of cases. Given that there was a limited number of cases in each facility, future research should involve collaboration with multiple facilities.

In conclusion, this study investigated the influence on the performance of a target model trained with a different type of lesion. This study showed that using different lesions for transfer learning improves the performance of the model.

Conflicts of Interest: None

Acknowledgements

We thank Helen Jeays, BDSc AE from Edanz (https://jp.edanz.com/ac) for editing a draft of this manuscript.

References

1. Kim HG, Lee KM, Kim EJ, Lee JS. Improvement diagnostic accuracy of sinusitis recognition in paranasal sinus X-ray using multiple deep learning models. Quant Imaging Med Surg 2019; 9: 942-51.
2. Murata M, Ariji Y, Ohashi Y, Kawai T, Fukuda M, Funakoshi T, et al. Deep-learning classification using convolutional neural network for evaluation of maxillary sinusitis on panoramic radiography. Oral Radiol 2019; 35: 301-7.
3. Nishiyama M, Ishibashi K, Ariji Y, Fukuda M, Nishiyama W, Umemura M, et al. Performance of deep learning models constructed using panoramic radiographs from two hospitals to diagnose fractures of the mandibular condyle. Dentomaxillofac Radiol 2021; 50: 20200611.
4. Lee A, Kim MS, Han SS, Park P, Lee C, Yun JP. Deep learning neural networks to differentiate Stafne's bone cavity from pathological radiolucent lesions of the mandible in heterogeneous panoramic radiography. PLoS One 2021; 16: e0254997.
5. Kise Y, Ikeda H, Fujii T, Fukuda M, Ariji Y, Fujita H, et al. Preliminary study on the application of deep learning system to diagnosis of Sjögren's syndrome on CT images. Dentomaxillofac Radiol 2019; 48: 20190019.
6. Kise Y, Shimizu M, Ikeda H, Fujii T, Kuwada C, Nishiyama M, et al. Usefulness of a deep learning system for diagnosing Sjögren's syndrome using ultrasonography images. Dentomaxillofac Radiol 2020; 49: 20190348.
7. Ariji Y, Fukuda M, Kise Y, Nozawa M, Yanashita Y, Fujita H, et al. Contrast-enhanced computed tomography image assessment

of cervical lymph node metastasis in patients with oral cancer by using a deep learning system of artificial intelligence. Oral Surg Oral Med Oral Pathol Oral Radiol 2019; 127: 458-63.
8. Yang H, Jo E, Kim HJ, Cha IH, Jung YS, Nam W, et al. Deep learning for automated detection of cyst and tumors of the jaw in panoramic radiographs. J Clin Med 2020; 9: 1839.
9. Watanabe H, Ariji Y, Fukuda M, Kuwada C, Kise Y, Nozawa M, et al. Deep learning object detection of maxillary cyst-like lesions on panoramic radiographs: preliminary study. Oral Radiol 2021; 37: 487-93.
10. Kuwana R, Ariji Y, Fukuda M, Kise Y, Nozawa M, Kuwada C, et al. Performance of deep learning object detection technology in the detection and diagnosis of maxillary sinus lesions on panoramic radiographs. Dentomaxillofac Radiol 2021; 50: 20200171.
11. Kuwada C, Ariji Y, Kise Y, Funakoshi T, Fukuda M, Kuwada T, et al. Detection and classification of unilateral cleft alveolus with and without cleft palate on panoramic radiographs using a deep learning system. Sci Rep 2021; 11: 16044.
12. Ariji Y, Fukuda M, Nozawa M, Kuwada C, Goto M, Ishibashi K, et al. Automatic detection of cervical lymph nodes in patients with oral squamous cell carcinoma using a deep learning technique: a preliminary study. Oral Radiol 2021; 37: 290-6.
13. Simonyan K, Zisserman A. Very deep convolutional networks for large-scale image recognition. The 3rd International Conference on Learning Representations; 2015 May 7-9; San Diego, California, USA. Available from: https://arxiv.org/abs/1409.1556.
14. Szegedy C, Liu W, Jia Y, Sermanet P, Reed S, Anguelov D, et al. Going deeper with convolutions. 2015 IEEE Conference on Computer Vision and Pattern Recognition; 2015 Jun 7-12; Boston, Massachusetts, USA. P. 1-9. Available from: https://arxiv.org/abs/1409.4842.
15. Mohammadi R, Salehi M, Ghaffari H, Rohani AA, Reiazi R. Transfer learning-based automatic detection of coronavirus disease 2019 (COVID-19) from chest X-ray images. J Biomed Phys Eng 2020; 10: 559-68.
16. Mori M, Ariji Y, Katsumata A, Kawai T, Araki K, Kobayashi K, et al. A deep transfer learning approach for the detection and diagnosis of maxillary sinusitis on panoramic radiographs. Odontology 2021; 109: 941-8.
17. Ishibashi K, Ariji Y, Kuwada C, Kimura M, Hashimoto K, Umemura M, et al. Efficacy of a deep leaning model created with the transfer learning method in detecting sialoliths of the submandibular gland on panoramic radiography. Oral Surg Oral Med Oral Pathol Oral Radiol 2022; 133: 238-44.
18. Ariji Y, Yanashita Y, Kutsuna S, Muramatsu C, Fukuda M, Kise Y, et al. Automatic detection and classification of radiolucent lesions in the mandible on panoramic radiographs using a deep learning object detection technique. Oral Surg Oral Med Oral Pathol Oral Radiol 2019; 128: 424-30.
19. Tao A, Barker J, Sarathy S. DetectNet: deep neural network for object detection in DIGITS. [updated 2016 Aug 11; cited 2022 July 25]. In: NVIDIA Developer. Technical Bog [Internet]. Santa Clara: NVIDA. Available from: URL: https://developer.nvidia.com/blog/detectnet-deep-neural-network-object-detection-digits/.
20. Barker J, Prasanna S. Deep learning for object detection with DIGITS. [updated 2016 Aug 11; cited 2022 July 25]. In: NVIDIA Developer. Technical Bog [Internet]. Santa Clara: NVIDA. Available from: https://developer.nvidia.com/blog/deep-learning-object-detection-digits/.
21. Koivisto T, Bowles WR, Rohrer M. Frequency and distribution of radiolucent jaw lesions: a retrospective analysis of 9,723 cases. J Endod 2012; 38: 729-32.
22. Robinson RA. Diagnosing the most common odontogenic cystic and osseous lesions of the jaws for the practicing pathologist. Mod Pathol 2017; 30(s1): S96-103.
23. Yeung AW. Radiolucent lesions of the jaws: an attempted demonstration of the use of co-word analysis to list main similar pathologies. Int J Environ Res Public Health 2022; 19: 1933.
24. Avril L, Lombardi T, Ailianou A, Burkhardt K, Varoquaux A, Scolozzi P, et al. Radiolucent lesions of the mandible: a pattern-based approach to diagnosis. Insights Imaging 2014; 5: 85-101.
25. Liu Z, Liu J, Zhou Z, Zhang Q, Wu H, Zhai G, et al. Differential diagnosis of ameloblastoma and odontogenic keratocyst by machine learning of panoramic radiographs. Int J Comput Assist Radiol Surg 2021; 16: 415-22.
26. Ariji E, Fujiwara N, Tabata O, Nakayama E, Kanda S, Shiratsuchi Y, et al. Stafne's bone cavity. Classification based on outline and content determined by computed tomography. Oral Surg Oral Med Oral Pathol 1993; 76: 375-80.
27. Estai M, Tennant M, Gebauer D, Brostek A, Vignarajan J, Mehdizadeh M, et al. Deep learning for automated detection and numbering of permanent teeth on panoramic images. Dentomaxillofac Radiol 2022; 51: 20210296.